Algal Research 92 (2025) 104417

Contents lists available at ScienceDirect

Algal Research

journal homepage: www.elsevier.com/locate/algal

# Influence of operational parameters on the performance of domestic wastewater treatment in a single-stage algal-bacterial column photobioreactor

Thalita Lacerda dos Santos [a,b], Laura Vargas-Estrada [a], Saúl Blanco [c], Gustavo Henrique Ribeiro da Silva [b], Raúl Muñoz [a,*]

[a] Institute of Sustainable Processes, University of Valladolid, Dr. Mergelina s/n., 47011, Valladolid, Spain
[b] São Paulo State University, Av. Eng. Luiz Edmundo C. Coube 14-01, 17033-360, Bauru, SP, Brazil
[c] University of León, Avenida de la Facultad, 25, 24004, León, Spain

ARTICLE INFO

*Keywords:*
Biomass productivity
Hydraulic retention time
Light availability
Microalgal-bacterial symbiosis
Solid retention time

ABSTRACT

This study evaluated the performance of a single-stage photobioreactor (PBR), under varying hydraulic retention times (HRT) (4, 3 and 2 days), biomass concentrations (2.7 and 1.6 gTSS $L^{-1}$) and illuminated surface/volume ratios (17.8 and 26.7 $m^2$ $m^{-3}$) in a continuous system operated for 192 days. The system achieved removal efficiencies of Total Organic Carbon of 94–96 %, Total Nitrogen of 92–97 % and phosphate of 91–100 % regardless of the operational conditions. N-$NH_4^+$ removal was primarily driven by assimilation into algal-bacterial biomass. Nitrate and nitrite accumulation in the cultivation broth was not observed and $N_2O$ generation was negligible. Increased light availability boosted biomass productivity up to 335.7 ± 77.8 g $m^{-3}$ $d^{-1}$. The reduction in biomass concentrations from 2.7 to 1.6 gTSS $L^{-1}$ decreased microalgal concentration and diversity, particularly affecting filamentous bacteria. These results demonstrate that a single-stage PBR can achieve performance comparable to conventional two stages anoxic-aerobic photobioreactors, while being more cost-effective and sustainable, highlighting its potential for advanced wastewater treatment and resource recovery.

## 1. Introduction

As anthropogenic activities drive global biogeochemical cycles beyond sustainable thresholds, domestic wastewater has emerged as a critical challenge for water security due to the complex mixture of organic matter, nutrients (e.g., nitrogen and phosphorus), pathogens, heavy metals and emerging pollutants including pharmaceuticals, personal care products, surfactants, pesticides, plasticizers, and others [1–6]. Conventional technologies treating domestic wastewaters such as activated sludge systems are often limited by high energy consumption associated with mechanical aeration and may achieve incomplete nutrient removal (e.g., 90–95 % nitrogen and 20–40 % phosphorus removal without tertiary treatment) [1,7–9]. These limitations are linked to the multi-stage configuration typically required for advanced nutrient removal (e.g., sequential processes like nitrification, denitrification, and phosphorus precipitation) [2,10,11].

In contrast, algae-bacteria technologies have emerged as a promising alternative, leveraging symbiotic microbial relationships for more sustainable wastewater treatment, to reduce aeration needs, enhance nutrient recover, and produce valuable biomass [1,12–14]. However, their net energy balance can be compromised by the energy requirements for mixing, and particularly by the energy-intensive harvesting of biomass [10,15].

Despite these challenges, microalgae-bacteria consortia remain a promising platform for wastewater treatment. In this symbiotic system, microorganisms play complementary roles for simultaneous carbon and nitrogen removal [15]. The process is based on bacterial oxidation of organic carbon and the conversion of nitrogen compounds, producing $CO_2$. This $CO_2$ is then utilized by photoautotrophic microalgae, which in return provide $O_2$ through photosynthesis. This synergy can eliminate the need for external aeration and chemical precipitation of phosphorus [11,16,17]. Additionally, the process facilitates phosphorus recovery primarily through assimilation into the microbial biomass, and generates a valuable biomass that can be used as a feedstock for bioproducts manufacture a soil amendment or biostimulant, restoring the nutrient cycle and improving crop productivity [1,3,18].

* Corresponding author.
*E-mail address:* raul.munoz.torre@uva.es (R. Muñoz).

https://doi.org/10.1016/j.algal.2025.104417
Received 7 September 2025; Received in revised form 29 October 2025; Accepted 3 November 2025
Available online 7 November 2025

Typically, studies assessing the performance of algal-bacterial consortia for wastewater treatment have been carried out in open photobioreactor such as high-rate algal ponds (HRAP), which can suffer from low photosynthetic efficiencies and nutrient removal [1,12,19]. In contrast, closed photobioreactors represent a suitable configuration to enhance the efficiency of microalgae-bacteria based wastewater treatment systems due to their larger illuminated surface area to volume ratio, better control of operational parameters, and higher biomass productivity [10,12,18,20]. This superior potential has been evidenced by Arbib et al. [21], who performed a direct comparison between a HRAP and an airlift tubular photobioreactor (TPBR) treating urban wastewater. The TPBR achieved significantly higher nutrient removal efficiencies (89 % TN and 86 % TP removal) compared to the HRAP (65 % TN and 58 % TP removal). This enhanced performance was concomitant with a substantially higher biomass areal productivity, which reached 21.8 gSS $m^{-2}$ $d^{-1}$ in the TPBR, compared to 8.3 gSS $m^{-2}$ $d^{-1}$ in the HRAP [21]. Nevertheless, closed PBRs still face challenges in optimizing operational parameters to maximize both microalgae growth and nutrient removal efficiency [18,19].

The HRT and SRT critically influence the balance between biomass activity and productivity [22,23]. Selecting appropriate values is essential for maintaining cells in their exponential growth phase, which optimizes both biomass productivity and carbon/nutrient removal efficiency [10]. The choice of these values is a key operational decision that must be tailored to the specific system, taking into account ambient conditions, nutrient availability, and reactor design [22]. Notably, Meng et al. [23] studied the influence of the SRT in the simultaneous nitrification-denitrification and phosphorous removal in a sequencing batch reactor. The authors demonstrated that a 15-day SRT achieved over 98 % of phosphorus and 85 % of nitrogen removal, primarily through nitrification-denitrification, while shorter SRT (5–10 days) favoured assimilation as the dominant process. This finding supports the approach of our study, as it confirms that manipulating the SRT is a viable strategy to shift the dominant nitrogen removal pathway towards assimilation.

Moreover, the light intensity can affects algal photosynthesis, bacterial nitrification, and biological community structure [3,24,25]. While high light intensities (>450 μmol $m^{-2}$ $s^{-1}$) can induce photoinhibition in both microalgae and nitrifying bacteria, this effect can be relevant for single-stage systems, where controlled nitrite oxidizing bacteria (NOB) inhibition creates a carbon-efficient shortcut for nitrogen removal via nitrite, an effect that can be balanced by operating at high biomass concentrations [3,11,23,24]. In this context, the literature reports photobioreactors operation under a wide range of biomass concentration, ranging from 0.1 to 8 gTSS $L^{-1}$. Unfortunately, high biomass concentrations (>2 gTSS $L^{-1}$) should be avoided to prevent detrimental self-shading effects [9,10]. On the other hand, biomass productivity ranging between 295.6 and 343.5 g $m^{-3}$ $d^{-1}$ have been achieved under different production strategies in an outdoor TPBR treating synthetic wastewater [19]. Nonetheless, gaps remain regarding in understanding the interplay of these key parameters on the overall performance of single-stage algal-bacterial photobioreactor. A systematic study investigating their combined effect is lacking.

In this context, this study aims to bridge this gap by evaluating the effect of the HRT, biomass concentration and illuminated surface area to volume ratio on the performance of carbon, nitrogen and phosphorous removal in a single-stage algal-bacterial column photobioreactor during domestic wastewater treatment. In addition, the impact of these operational parameters on the microalgae population structure was assessed. The experimental design herein proposed was specifically intended to fill the above mentioned research gap by testing a matrix of these key parameters to map their individual and combined effects on system performance, thereby identifying the most promising conditions for efficient nutrient removal via assimilation.

## 2. Materials and methods

### 2.1. Inoculum

The inoculum consisted of a mixture of concentrated microalgae-bacteria consortium and fresh aerobic activated sludge (AS). The AS was collected from the activated sludge secondary settler of Valladolid wastewater treatment plant (WWTP), with a total suspended solids (TSS) concentration of 4.2 g $L^{-1}$.

The algal-bacterial consortium was obtained from an indoor HRAP treating real centrate from the same WWTP as described elsewhere [26]. This consortium was predominantly composed of filamentous bacteria (80 % of the community) and 20 % of *Mychonastes homosphaera* morphotype and was concentrated by centrifugation (4000 rpm, 15 min), removing the supernatant, and mixing the resulting biomass pellet with the AS broth. The mixture was then resuspended in synthetic wastewater (SWW) to reach a final volume of 22 L, achieving an initial total suspended solids (TSS) concentration of 1.8 g $L^{-1}$.

### 2.2. Synthetic wastewater composition

The SWW was prepared to minimize fluctuations in composition and to maintain stable operating conditions. The SWW was prepared based on the BG 11 medium adapted from Ferro et al. [27] using tap water. The composition of the SWW was (per L): 0.625 g glucose, 0.7 g $NaHCO_3$, 0.16 g peptone, 0.11 g meat extract, 0.15 g $NH_4Cl$, 0.04 g $K_2HPO_4$, 0.075 g $MgSO_4.7H_2O$, 0.036 g $CaCl_2.2H_2O$, 0.02 g $Na_2CO_3$ and 1 mL of micronutrients solution composed of (per L): 6.0 g citric acid, 6.0 g ferric ammonium citrate, 1.0 g EDTA.$Na_2$, 2.86 g $H_3BO_3$, 1.81 g $MnCl_2.4H_2O$, 0.39 g $Na_2MoO_4.2H_2O$, 0.08 g $CuSO_4.5H_2O$, 0.05 g $Co(NO_3)_2.6H_2O$, 0.22 g $ZnSO_4.7H_2O$. This resulted in a pH of 8.1 ± 0.3, 368.3 ± 28.5 mg $L^{-1}$ of total organic carbon (TOC), 135.2 ± 12.1 mg $L^{-1}$ of inorganic carbon (IC), 72.6 ± 5.2 mg $L^{-1}$ of total nitrogen (TN), and 18.5 ± 1.6 mg $L^{-1}$ of phosphorus (P-$PO_4^{3-}$), which corresponded to a C:N:P mass ratio of 20:4:1.

### 2.3. Experimental set-up

The experimental setup consisted of a column photobioreactor (PBR) with a working volume of 22 L (0.15 m of diameter and 1.31 m height). The PBR was divided into two functional zones: an illuminated zone and a light-shielded zone (Fig. 1). The light-shielded zone was created by enclosing the bottom part of the PBR with a black cardboard shield, corresponding to one-third of the total height of the liquid. The average light intensity inside the PBR was calculated using a light attenuation model [28]. The reduction in the light flux corresponding to covering 1/3 of the PBR surface would entail a reduction from 21 μmol $s^{-1}$ (Stage V) to 8–12 μmol $s^{-1}$ (Stage I-IV), as detailed in Table 1. To ensure continuous agitation of the cultivation broth of the PBR, one pump was installed at the bottom (Eden 159, Eden WaterParadise, Spain) and a second pump was installed in the upper third part of the PBR (CompactON 300, Eheim, Spain).

The PBR was continuously illuminated by two LED PCBs panels (Philips S.A., Poland), arranged vertically in opposite sides of the reactor, providing an average light intensity of 431 ± 18 μmol $m^{-2}$ $s^{-1}$. Continuous illumination was chosen to establish consistent and reproducible baseline conditions, eliminating the variability introduced by light-dark cycles as an additional factor of variability. The available illuminated surface area varied throughout the experiment: 0.39 $m^2$ during the first four stages, and 0.59 $m^2$ during Stage V.

The PBR was connected to a 1 L conical settler, which allowed to recirculate a fraction of the settled biomass to the PBR at a flow rate of 0.75 L $d^{-1}$, and to daily withdrawn biomass to control the solid retention time (SRT). The experimental period was extended to 192 days.

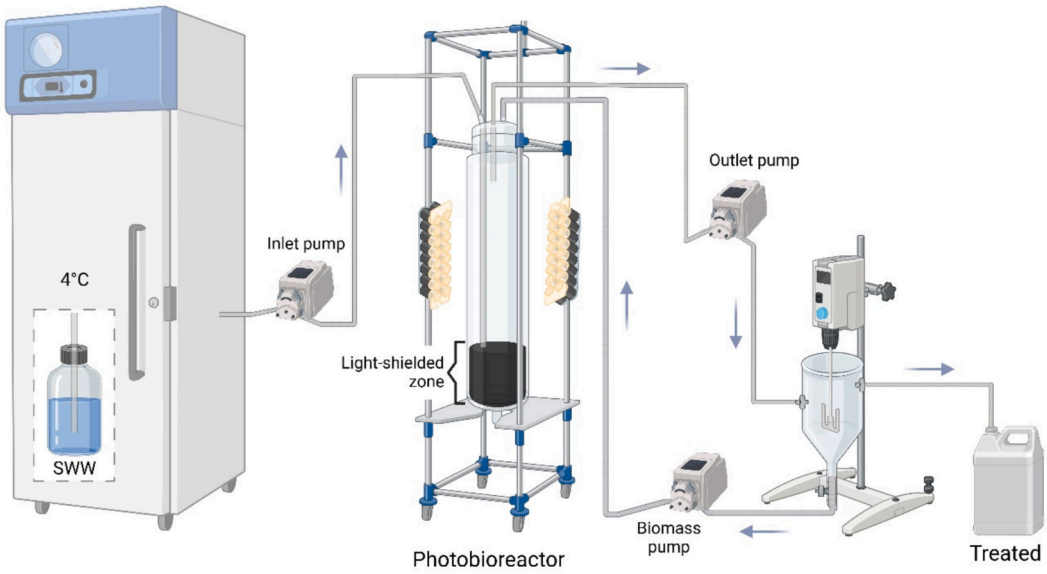


**Fig. 1.** Schematic diagram of the experimental set-up.

**Table 1**
Operational conditions and process parameters during the evaluation of the performance of the PBR.

| | Stage I | Stage II | Stage III | Stage IV | Stage V |
|---|---|---|---|---|---|
| Period (d) | 36 | 31 | 21 | 41 | 18 |
| HRT (d) | 4 | 3 | 2 | 2 | 2 |
| SRT (d) | 11 ± 2 | 10 ± 2 | 10 ± 1 | 3 ± 1 | 3 ± 1 |
| Illuminated area S ($m^2$) | 0.39 | 0.39 | 0.39 | 0.39 | 0.59 |
| Surface light intensity (μmol $m^{-2}$ $s^{-1}$) | | | 431 ± 18 | | |
| S/V ($m^2$ $m^{-3}$) | 17.8 | 17.8 | 17.8 | 17.8 | 26.7 |
| Average internal light flux (μmol $s^{-1}$) | 8 | 7 | 8 | 12 | 21 |

### 2.4. Operational conditions and sampling procedures

The experiment was divided into five operational stages. The initial 45-day period was devoted to system stabilization until steady state conditions were achieved. The HRT was selected based on Alcántara et al. [29]. During Stage I, the system was operated for 36 days at an HRT of 4 days. In Stage II, the HRT was reduced to 3 days, which was maintained for 31 days. During Stage III (21 days of operation), the HRT was further reduced to 2 days. An initial SRT of 10 days was chosen based on previous literature studies to ensure community stability [25]. In Stage IV (HRT = 2 days), the biomass concentration in the PBR was maintained below 2 gTSS $L^{-1}$ by centrifuging a certain volume of the culture, withdrawing the biomass pellet, and returning the supernatant to the PBR. This operational shift reduced SRT from 10 to 3 days. Stage IV was operated for 41 days. Finally, the black cardboard shield was removed in Stage V and the operating conditions were kept similar to Stage IV, for 18 days. The operational conditions set in this experiment are summarized in Table 1.

The pH, dissolved oxygen (DO), and temperature were daily monitored at 11:00 am. Twice a week, liquid samples of 100 mL were withdrawn from the SWW, the PBR and the effluent of the settler to measure the concentration of IC, TOC, TN, N-$NH_4^+$, N-$NO_2^-$, N-$NO_3^-$, and P-$PO_4^{3-}$. The concentration of TSS and volatile suspended solids (VSS) was determined in the PBR, bottom of settler and effluent of the settler. The concentration of $N_2O$ in the headspace of the PBR was measured in duplicate by collecting 100 μL of gas samples twice a week. Additionally, samples from the culture broth of the PBR were collected at the end of each operational stage to determine the structure of population of microalgae.

### 2.5. Analytical procedures

#### 2.5.1. Standard physicochemical parameters

The pH was measured with a SensION™ + PH3 pHmeter (HACH, The Netherlands). The temperature inside the PBR was monitored with a multiparameter analyser C-3020 (Consort, Belgium) and DO was monitored using an OXI 3310 oximeter (WTW, Germany). The photosynthetic active radiation (PAR) at the PBR walls was measured with a LI-250A light meter (LI-COR Biosciences, Germany). TSS and VSS concentrations were measured according to Standard Methods [30].

#### 2.5.2. Liquid phase analysis

Samples for liquid analysis were filtered through 0.45 μm membranes prior to analysis. Dissolved TOC, IC and TN concentrations were determined using a Shimadzu TOC-VCSH analyser (Japan) equipped with a TNM-1 chemiluminescence module, dilution were needed only for SWW. N-$NH_4^+$ concentration was determined by the Nessler method. Briefly, appropriated dilution of the filtered samples was reacted with Nessler reagent. After 10-min reaction time, the absorbance was measured using a Shimadzu UV-2550 spectrophotometer (Japan) at a wavelength of 425 nm. A calibration curve was prepared using standard ammonium solutions within a range of 0.1 to 10 mgN $L^{-1}$. The concentration of N–$NO_2^-$, N–$NO_3^-$, and P-$PO_4^{3-}$ were quantified by HPLC-IC (Waters 432, conductivity detector, USA).

#### 2.5.3. Gas phase analysis

$N_2O$ was collected from gas sampling septum on the top of the PBR and determined with a gas chromatograph (Bruker Scion 436, Palo Alto, USA) equipped with an Electron Capture Detector and a HS-Q packed column according to Frutos et al. [31].

#### 2.5.4. Biomass characterization

The determination of C, H, N, S and O content of the microalgae biomass was carried out from freeze-dried biomass with an elemental analyser EA Flash 2000, Thermo Fisher Scientific. The identification and quantification of the microalgae consortium was conducted by microscopy examination (OLYMPUS IX70, USA) from samples fixed with Lugol (5 % *v*/v) and formaldehyde solution at (10 % v/v). The samples

were stored at −20 °C until the analysis was performed.

### 2.6. Calculations

The biomass productivity (BP) (g $m^{-3}$ $d^{-1}$) set via harvesting from the settler was determined according to Eq. (1) [22]:

$$BP = \frac{(Q_{wastage} \times TSS) + (Q_{out} TSS_{out})}{V_{PBR}} \quad (1)$$

where $Q_{wastage}$ is the wastage flowrate withdrawn from the bottom of the settler (L·$d^{-1}$); $Q_{out}$ is the effluent flowrate from the outlet of the settler (L·$d^{-1}$); $TSS$ is the biomass concentration of the $Q_{wastage}$ (g·$L^{-1}$); $TSS_{out}$ is the biomass concentration of the effluent and $V_{PBR}$ is the volume of the PBR ($m^3$).

The nutrient removal efficiency (NRE) was calculated according to Eq. 2:

$$NRE_i = \frac{C_{SWW} - C_{out}}{C_{SWW}} \times 100 \quad (2)$$

where $NRE_i$ represents the removal efficiency (%) of the parameter *i* (TOC, IC, TN, N-$NH_4^+$ and P-$PO_4^{3-}$), $C_{SWW}$ is the concentration of the parameter *i* in the SWW and $C_{out}$ is the concentration of the parameter *i*

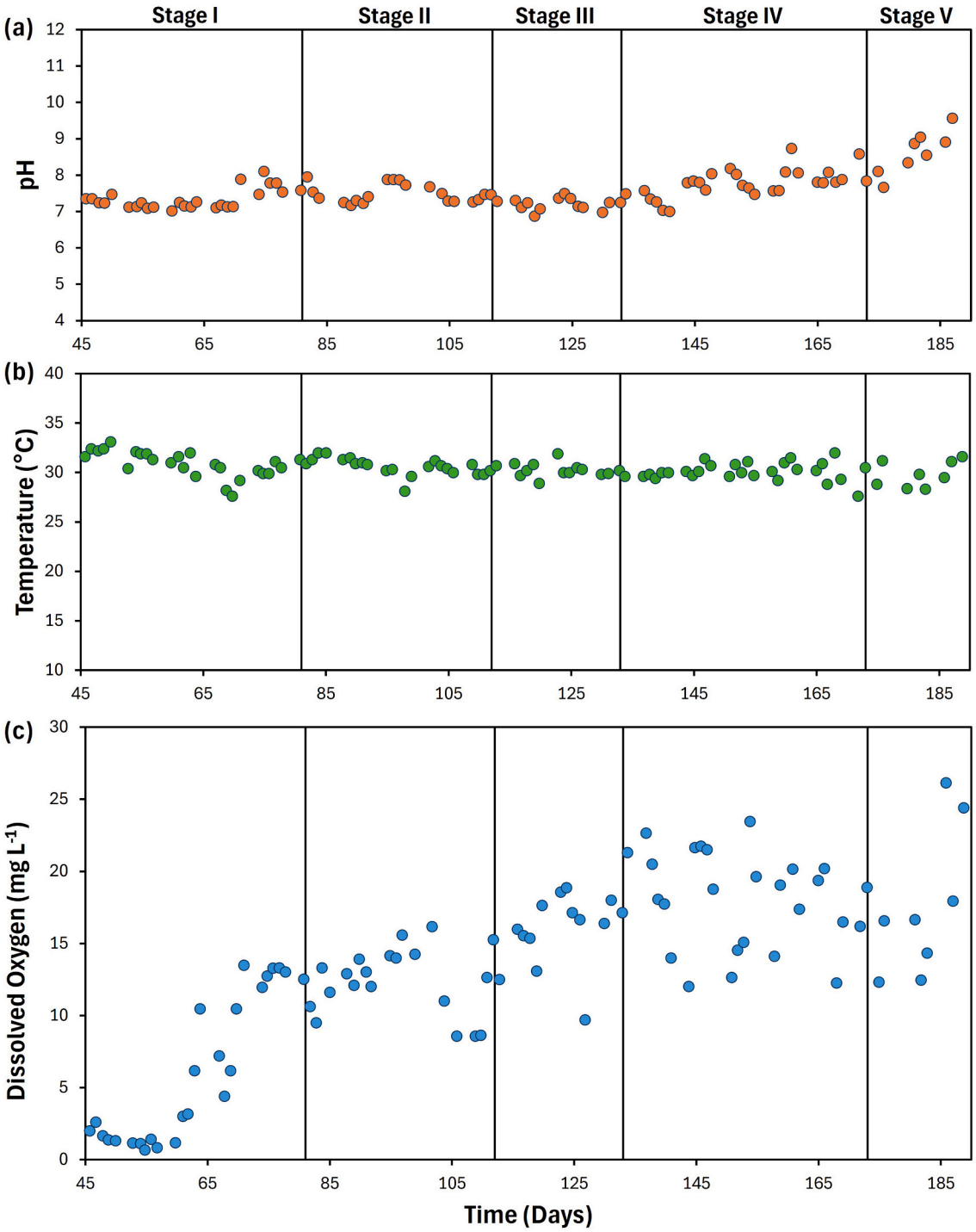


**Fig. 2.** Time course of the (a) pH, (b) temperature and (c) dissolved oxygen concentration in the algal-bacterial broth during PBR operation.

in the effluent of the settler. Mass balance calculation was conducted for TOC, IC, TN, N-$NH_4^+$ and P-$PO_4^{3-}$, in each operational stage.

The nitrogen mass balance was calculated according to Eq. 3 [32]:

$$Q_{in} \bullet TN_{in} = \left(V_{PBR} \bullet BP \bullet \frac{\%N}{100}\right) + (Q_{out} \bullet TN_{out}) + (N_{loss}) \quad (3)$$

where $Q_{in}$ is the flow rate of the inlet SWW (L $d^{-1}$); $TN_{in}$ is the total nitrogen concentration in the inlet SWW (g $L^{-1}$); $V_{PBR}$ is the reactor volume ($m^3$); $BP$ is the biomass productivity (g $m^{-3}$ $d^{-1}$); $\%N$ is the nitrogen content in the biomass (%); $Q_{out}$ is the flow rate of the effluent (L $d^{-1}$); $TN_{out}$ is the total nitrogen concentration in the effluent (g $L^{-1}$) and $N_{loss}$ represents the unaccounted nitrogen in the mass balance, calculated as the closing term. The $N_{loss}$ was calculated as the difference between the TN input and the sum of TN in the effluent and the N recovered in the biomass.

### 2.7. Data analysis and visualization

Schematic figures, including Graphical Abstract and Fig. 1, were created using BioRender.com.

The results are presented as the mean values ± standard deviation for each parameter, calculated during steady state. Data normality was assessed using the Shapiro-Wilk and Kolmogorov-Smirnov tests. Statistical comparisons were performed using Student's *t*-test, one-way ANOVA, and Tukey's post-hoc test, with all analyses conducted in the Jamovi software (version 2.3.28).

## 3. Results and discussion

### 3.1. Evolution of environmental parameters during photobioreactor performance

Temperature, DO, and pH were periodically monitored throughout the experiment. Throughout Stage I to III the pH remained stable and averaged 7.4 ± 0.3 (Fig. 2a). Interestingly, the decrease in biomass concentration in Stage IV enhanced microalgae photosynthetic activity, and the pH increased up to 7.8 ± 0.4 ($p < 0.05$). This increasing pH trend continued in Stage V up to an average pH of 8.6 ± 0.6. No external control was required to maintain the pH in the algal-bacterial broth, demonstrating that under the tested conditions, the pH stability and subsequent increase suggest a net dominance of $CO_2$-consuming processes, such as photosynthesis, over acidifying processes like nitrification.

The temperature of the cultivation broth remained stable (30 ± 1 °C) throughout all stages (Fig. 2b). On the other hand, DO levels increased progressively across operational stages, likely due to enhanced photosynthetic activity in spite of the increasing oxygen demand when decreasing the HRT. Thus, DO concentrations remained <3 mg O $L^{-1}$ for the first 14 days of Stage I, likely due to the low biomass concentration and low photosynthetic activity of a microalgal-bacterial consortium acclimating to the environmental and operational conditions in the photobioreactor. The subsequent rise in DO, reaching values >12 mg $O_2$ $L^{-1}$ in Stage V, is a consequence of the enhanced photosynthetic activity associated with the increased in IC removal (Fig. 3), which was driven by the higher light intensity provided. The oxygen production from this intensified photosynthesis far exceeded the residual oxygen demand for nitrification, leading to the oxygen accumulation observed.

### 3.2. Carbon and phosphorus removal

The PBR herein evaluated demonstrated a highly efficient organic carbon removal, consistently achieving TOC removal efficiencies above 94 ± 1 % across all operational stages at TOC loading rates ranging from 85 to 199 gTOC $m^{-3}$ $d^{-1}$ (Fig. 3). This performance is comparable to other single-stage algal bacterial systems treating municipal

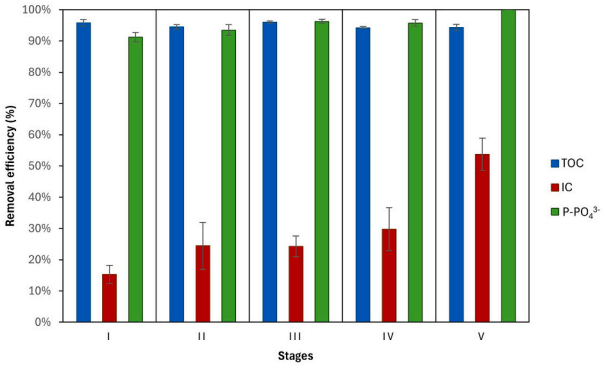


**Fig. 3.** Steady state TOC, IC and P-$PO_4^{3-}$ removal efficiencies during PBR operation.

wastewater. For instance, Aparicio et al. [33] reported COD removal efficiencies higher than 86 % in a membrane-assisted HRAP treating urban wastewater, while Arango et al. [34] achieved 92–98 % COD removal in 50 L raceways PBRs. Similarly, He et al. [35] reported TOC removal efficiencies of 65–98 % in a tubular PBR treating primary-treated municipal wastewater, while Posadas et al. [36] achieved 90 % TOC removal in a biofilm reactor treating domestic wastewater. On the other hand, the anoxic-aerobic configurations of Alcántara et al. [29] and Torres-Franco et al. [13] also achieved high TOC removal (85–96 %). Therefore, this study confirmed that single-stage configuration photobioreactors can achieve comparable organic matter removals than more complex two-stage systems.

This study demonstrated a strong correlation between microalgal activity and IC removal, as evidenced by the concurrent increase in both parameters following operational changes. The reduction of HRT in Stages I to III, which enhanced biomass productivity by 15 %, resulted in the IC removal rate increased from 4.6 to 16.7 mgIC $L^{-1}$ $d^{-1}$. This suggests that the photosynthetic activity was the primary driver of inorganic carbon assimilation. The reduction in biomass concentration in the PBR during Stage IV to 1.5 ± 0.4 gVSS $L^{-1}$, improved light penetration, subsequently increasing the average IC removal efficiency from 24 ± 3 % in Stage III up to 30 ± 7 %. This tendency was reinforced in Stage V, where the increased illuminated surface-to-volume ratio from 17.8 to 26.7 $m^2$ $m^{-3}$ in Stage V boosted light supply from 168 to 253 μmol $s^{-1}$. This increase, combined with the TOC was nearly completely removed (>94 % efficiency), create ideal conditions for photoautotrophy. Following the depletion of organic carbon source, a 750 % increase in IC removal rate compared to Stage I was observed, reaching 38.9 mg IC $L^{-1}$ $d^{-1}$, which far exceeded the relative increased in light availability, highlights a significant metabolic shift within the system in response to the changing carbon availability. It is important to note that this IC consumption was not solely due to microalgae; other processes like nitrification also contributed to the overall removal.

Steady state P-$PO_4^{3-}$ removal efficiencies reached 96 ± 1 % in Stages III and IV, and increased up to 100 % in Stage V (Fig. 3). In this context, the SWW herein used exhibited a N:P molar ratio of 26:1, which is higher than the optimal ratio of 11:1 recommended by Karemore et al. [12] for promoting algal cell growth. While phosphorous deficiency can hinder the growth of nitrifying bacteria, it does not significantly affect microalgae due to their ability to perform luxury uptake [22]. Additionally, since pH values remained below 10 and these conditions do not support phosphate precipitation, it can be inferred that the high phosphorous removal efficiency observed in this study was primarily driven by phosphorous assimilation into biomass, aligning with the recent findings of Torres-Franco et al. [13].

### 3.3. Nitrogen removal

The TN removal efficiency increased from 92 ± 6 % in Stage I to 98

± 1 % in Stage V (Fig. 4a). TN removal was directly linked to assimilation into new biomass [10]. This process primarily depends on light availability and IC supply during photosynthetic growth, although heterotrophic metabolism can also contribute to biomass formation [10]. The N content in microalgae typically ranges from 6.6 % to 9.3 % [10] and in this study, varied from 7.4 ± 0.4 % to 8.7 ± 0.3 %, with the highest value observed in Stage III. This effective TN removal was the result of an active $NH_4^+$ uptake, which consistently exceeded 98 % across all stages (Fig. 4b), mainly driven by the low energy requirements for ammonium microalgae assimilation [22]. The biomass composition remained consistent across all stages, with an empirical composition of $CH_{1.8}O_{0.5}N_{0.2}$. This consistency supports the assumption of a theoretical biomass composition of $CH_{1.7}O_{0.4}N_{0.2}P_{0.0094}$ [37], and suggests that, in this case, the changes in operational conditions did not significantly impact the biomass composition.

The ratio of total carbon removed to ammonium removed (mg $TOC_{removed}$/mg $N\text{-}NH_{4removed}^+$) averaged 7.3 ± 0.3 throughout the study, while the carbon to nitrogen ratio in the biomass (mg $C_{biomass}$/mg $N_{biomass}$) obtained from the elemental analysis was in average 6.1 ± 0.4. These results suggest that the primary mechanism of $N\text{-}NH_4^+$ removal was assimilation into algal-bacterial biomass, which was consistent with the findings of Alcántara et al. [29]. Interestingly, the step reduction in HRT conducted from Stage I to III did not significantly affect $NH_4^+$ concentration in the PBR ($p > 0.05$), consistent with findings by Buha et al. [38] operating two identical aerobic–anoxic sequencing bioreactors at high $N\text{-}NH_4^+$ concentrations.

It is important to highlight that the concentrations of $N\text{-}NO_2^-$ and $N\text{-}NO_3^-$ in the SWW fluctuated across the five operational stages due to variations in the characteristics of the tap water used for SWW preparation. The reduction in the HRT from Stages I to III increased $N\text{-}NO_2^-$ concentration in PBR from 0.3 ± 0.1 mg $L^{-1}$ to 0.6 ± 0.1 mg $L^{-1}$. Despite this increase, concentrations remained significantly lower than the 5 mg $L^{-1}$ reported in an algal-bacterial PBR treating SWW at an 8-days HRT [17]. During Stage III, nitrogen mass balance demonstrated that $N_{loss}$ peak at 40 % of total nitrogen removal, representing its highest contribution throughout the stages. Nonetheless, at this particular stage, the PBR exhibited the highest microalgal density ($9.28 \times 10^{10}$ ind $L^{-1}$; Fig. 6a) with filamentous bacteria comprising 59 % of the total microbial population, confirming the fact that biomass assimilation was still the primary nitrogen removal.

On the other side, the reduction of SRT, in our particular study, from 10 days (Stages I to III) to 3 days (Stages IV and V), associated to the decrease in biomass concentration from 2.7 ± 0.2 to 1.6 ± 0.2 gTSS $L^{-1}$, prevented the nitrate and nitrite accumulation. This can be attributed to the effective light penetration and potential inhibition of NOB under the prevailing conditions, preventing nitrite accumulation despite the relatively short SRT. Notably, $N\text{-}NO_2^-$ was undetectable in Stage V, suggesting that either complete nitrite oxidation by NOB or nitrite denitrification might have occurred [38]. Despite the high DO levels, the mass balance calculation for Stage V indicated a nitrogen loss of 25 % of the total nitrogen removal, with nitrogen assimilation dominating (0.55 gN $d^{-1}$), likely due to the enhanced microalgae and nitrifying bacterial activities. This aligns with the consistently high $N\text{-}NO_3^-$ removal efficiencies of 87 ± 1 % across all stages (Fig. 4c), driven by microalgal activity. This can be attributed to the nitrate uptake rate exceeding the ammonia nitrification rate [39].

Although the complex relationship between microalgae and bacterial consortia influences nutrient removal, nitrification is typically favoured by longer SRT, which allow the enrichment of nitrifying bacteria, while denitrification is primarily driven by the prevalence of anoxic conditions, achievable under various SRT and HRT conditions [33,34]. Whilst excessively short SRTs (e.g., <2 days) can lead to $NO_2^-$ accumulation due to a higher ammonia oxidizing bacteria (AOB) activity compared to the activity of microalgae and NOB, which can negatively impact microalgal performance [22]. The results obtained in this study indicated that the selected operational conditions effectively supported system stability, by preventing the accumulation of nitrogenous intermediates and promoting efficient removal.

Moreover, the increased illuminated area did not influence the nitrogen species assimilation as $N\text{-}NO_2^-$ remained undetectable in Stage V, despite the high sensitivity of NOB to excessive light intensity provided to the PBR, which exceeded the reported limit of tolerance of NOB >450 μmol $m^{-2}$ $s^{-1}$ [24]. Indeed, a prolonged light exposure can damage nucleic acids and chromophores in AOB and NOB, with NOB being more sensitive and AOB exhibiting a faster recovery and developing greater photoresistance [11]. Additionally, NOB are typically more light-sensitive than AOB, which can lead to partial nitrification and nitrite accumulation due to inhibition of the second nitrification step [22]. However, the $N\text{-}NO_3^-$ and $N\text{-}NO_2^-$ remained consistent in the PBR across all stages.

Finally, $N_2O$ emissions were monitored throughout all experimental stages, with measured concentrations of 2.11 mgN $L^{-1}$ in the headspace of the PBR, representing 0.1 % of the influent TN. These emissions were significantly lower than the typical 1.6 % of influent TN mass load used for environmental impact assessments of wastewater treatment [40], confirming its negligible impact on both greenhouse gas emissions and nitrogen mass balance of the system. It is important to highlight that $N_2O$ emissions were only detected in stages I-III, when the system was operated under an illuminated S/V ratio of 17.8 $m^2$ $m^{-3}$ and the microalgae concentration within the reactor was >2 gTSS $L^{-1}$, which could have significantly promoted self-shading effect and anoxic zones inside the cultivation broth. Interestingly, when the biomass concentration within the reactor was set below 2 gTSS $L^{-1}$, $N_2O$ emissions were not detectable. Thereby, the lower biomass concentration likely reduced the self-shading effect within the reactor, resulting in negligible $N_2O$ emissions from the microalgae-bacteria consortium. It has been recently demonstrated that microalgae can produce $N_2O$ under dark conditions and low DO levels [6,41]. However, the operational conditions imposed in this work (i.e. continuous illumination), along with the high photosynthetic microalgae activity recorded (DO >5 mg $L^{-1}$), suggest that $N_2O$ emissions were likely attributed to bacterial activity. $N_2O$ is an intermediate and byproduct of denitrification and nitrification processes, respectively [41], and is mainly produced from nitrite. Thereby, the presence of $NO_2^-$ in the reactor during Stages I to III can be attributed to the activity of aerobic AOB, and since no $NO_3^-$ accumulation within the reactor was observed, it could be suggested that simultaneous denitrification-nitrification was being carried out in the PBR.

### 3.4. Biomass productivity and microalgae populations

Despite the HRT reduction in Stages I to III, biomass productivity increased from 218.4 ± 22.6 to 250.6 ± 37.9 g $m^{-3}$ $d^{-1}$. Upon implementation of a more intensive biomass withdrawal strategy in Stages IV and V, which reduced the SRT to 3 days, biomass productivity increased up to 522.4 ± 126.9 g $m^{-3}$ $d^{-1}$ in Stage IV. This improvement can be attributed to diminished self-shading effects, enhanced nutrients availability for microalgae growth and increased biomass withdrawal rate, which maintained PBR concentration below 2 gTSS $L^{-1}$.

Increasing the S/V ratio to 26.7 $m^2$ $m^{-3}$ in Stage V reduced biomass productivity to 339.7 ± 70.1 g $m^{-3}$ $d^{-1}$, although statistical analysis indicated no significant difference between Stages IV and V. This result reveals that the biomass productivity was limited by microalgae physiological aspects resulting from the continuous illumination. Typically, during saturated illumination the photosynthetic rate reaches its maximum value and does not increase with increasing illumination [42]. Hence, the absence of a dark cycle, where microalgae could have recovered and improve their cell division in addition to the resulting oxygen supersaturation (>12 $mgO_2$ $L^{-1}$ in Stage V, Fig. 2) could have imposed an additional constraint, potentially inhibiting sensitive microbial populations within the consortium. In this context, the high dissolved oxygen concentrations prevailing during most of the

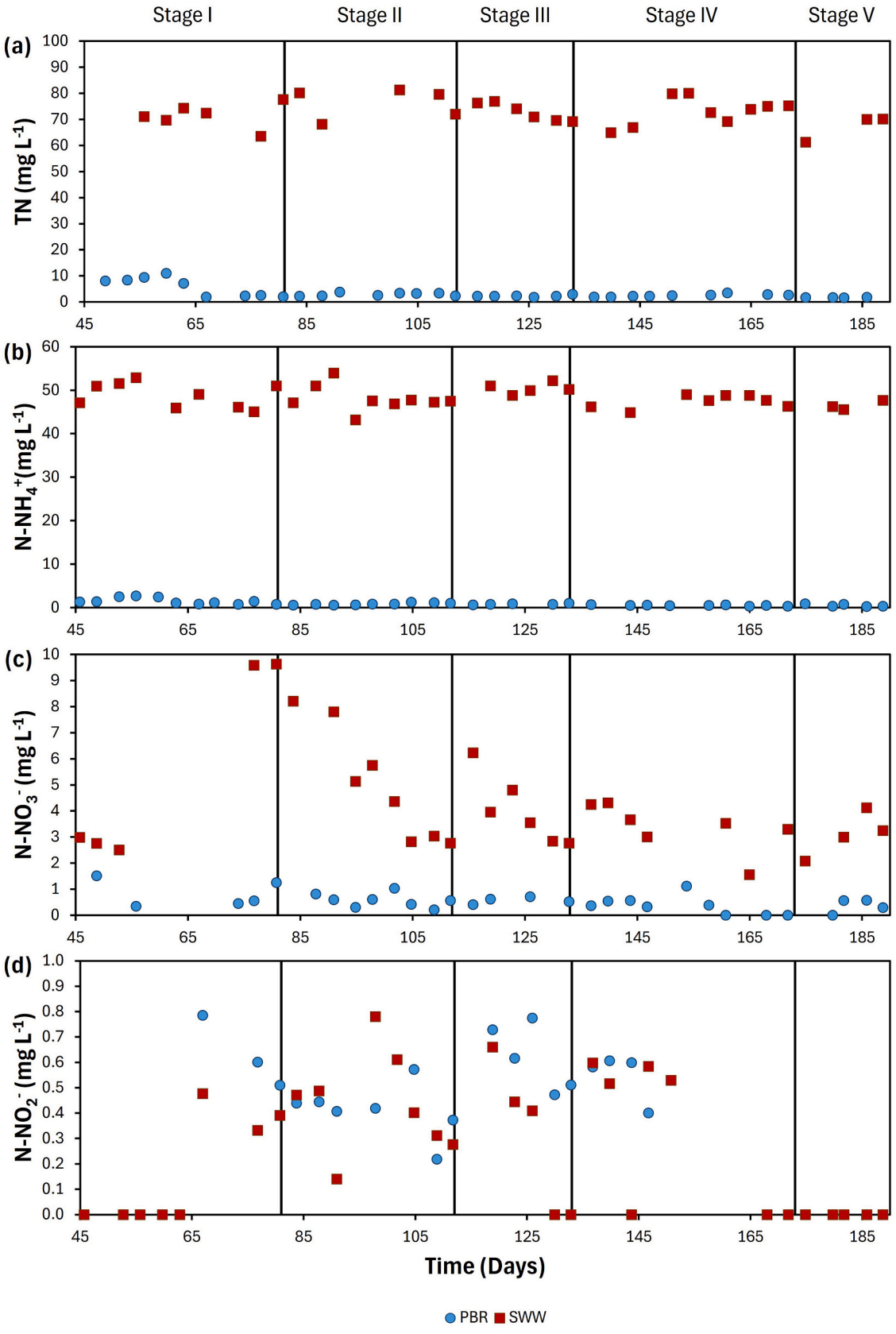


**Fig. 4.** Time course of the different nitrogen species a) Total nitrogen; b) $N\text{-}NH_4^+$; c) $N\text{-}NO_3^-$; and d) $N\text{-}NO_2^-$ in the cultivation of the PBR (blue circles) and in SWW (red squares) during the different operational stages. (For interpretation of the references to colour in this figure legend, the reader is referred to the web version of this article.)

experimental period might have induced the formation of reactive oxygen species (ROS) with potential to damage the photosynthetic system [42].

In outdoor systems, biomass production is fundamentally limited by the natural photoperiod. For instance, the optimized strategy in the outdoor TPBR studied by Andrade et al. [19] achieved a daily productivity of 257.8 g $m^{-3}$ $d^{-1}$, a value constrained by the hours of daylight. Therefore, while optimizing the S/V ratio remains crucial for light capture, this study demonstrates that its effectiveness is ultimately bounded by the physiological limits of the consortium.

Moreover, biomass concentration exhibited an inverse correlation with DO [43]. Thus, the reduction of average biomass concentrations from 2.7 ± 0.2 gVSS $L^{-1}$ in Stage III to 1.5 ± 0.3 gVSS $L^{-1}$ in Stage V (Fig. 5) resulting from increased biomass harvesting rates, were associated with higher DO levels (Fig. 2c). This increased DO concentration in addition to the high light intensity, could have induced the ROS formation, limiting microalgae growth.

The effluent TSS concentrations average 0.14 ± 0.06 g $L^{-1}$ throughout the study, corresponding to a biomass removal efficiency of 94 ± 3 % in the settler. Despite this high efficiency, this biomass concentration consistently exceeded the maximum TSS discharge limit established by the European Union Legislation (35 mg $L^{-1}$) (EU, 2024). Similar results were reported by Toledo-Cervantes et al. [44] in a pilot HRAP with biomass recirculation based on biomass productivity control, where TSS concentration of 70 ± 50 mg $L^{-1}$ also exceeded regulatory limits, demonstrating that increased biomass wastage rates could reduce TSS concentrations, while potentially enhancing photosynthetic efficiency. However, the limited sedimentation capacity of many microalgae species frequently leads to effluent with TSS levels that exceed the allowable discharge thresholds for natural water bodies [29].

Microscopic analysis of the microalgal-bacterial community, based on morphological identification, was conducted under stable operational performance, as each experimental stage was maintained for a period equivalent to at least 8 HRT prior to data collection, ensuring system stability. Under these conditions, the most frequently observed morphotypes in the PBR during the experimental stages belonged to three phyla and different classes: Chlorophyta (Green Algae), the class Chlorophyceae (including *Scenedesmus* morphotype, *Scenedesmus quadricauda* morphotype, and *Tetradesmus obliquus* morphotype) and the class Trebouxiophyceae (*Mychonastes homosphaera* morphotype and *Chloroidium ellipsoideum* morphotype); Bacillariophyta (Diatoms), the class Bacillariophyceae (*Nitzschia palea* morphotype); and Cyanobacteria (including *Pseudanabaena* morphotype and filamentous bacteria).

The initial high relative abundance of filamentous bacteria over microalgae (*Mychonastes homosphaera* morphotype) in the inoculum likely contributed to the low dissolved oxygen (DO <5 mg $L^{-1}$) observed during the first 14 days of operation (Fig. 2b). In Stage I, the decline in filamentous bacteria (48 % of total population), alongside an increase in the relative abundance of *Mychonastes homosphaera* morphotype (48 %), resulted in a reduced cell density but increased biovolume, reflecting the replacement of numerous small bacterial cells with fewer, larger microalgal cells. The colonial morphology of emergent species (*Tetradesmus obliquus* morphotype with 3 % and *Scenedesmus quadricauda* morphotype with 1 %) further enhanced the biovolume of the prevailing microbial community. The reduction of HRT in Stage II resulted in an increase in the relative abundance of *Mychonastes homosphaera* morphotype (53 %) and *Tetradesmus obliquus* morphotype (14 %) was observed, driving a 32 % biovolume increase and peak TSS (3.2 ± 0.4 g $L^{-1}$ on average), concomitant with a 11 % reduction in cell density versus Stage I. The disappearance of *Scenedesmus quadricauda* morphotype suggests potential competitive exclusion for nutrients (increased of IC and P-$PO_4^{3-}$; Fig. 3 and TN; Fig. 4a) under these conditions. Stage III (HRT = 2d) was characterized by a 127 % increase in cell density, primarily composed of filamentous bacteria morphotype (59 %). The observed microbial shift suggests that the reduction in HRT created selective pressure that favoured the proliferation of these bacterial morphotypes. This shift occurred alongside a reduced relative biovolume (6 $\mu m^3$ $cell^{-1}$), reflecting the substitution of larger microalgae (*Mychonastes homosphaera* morphotype: 40 %; *Tetradesmus obliquus* morphotype: 1 %) by smaller and numerous bacterial cells. The highest $N_{loss}$ observed in this stage, coupled with the increased relative abundance of bacterial morphotypes, suggests a period of intensified bacterial activity.

The biomass withdrawal strategy in Stage IV reduced microalgae

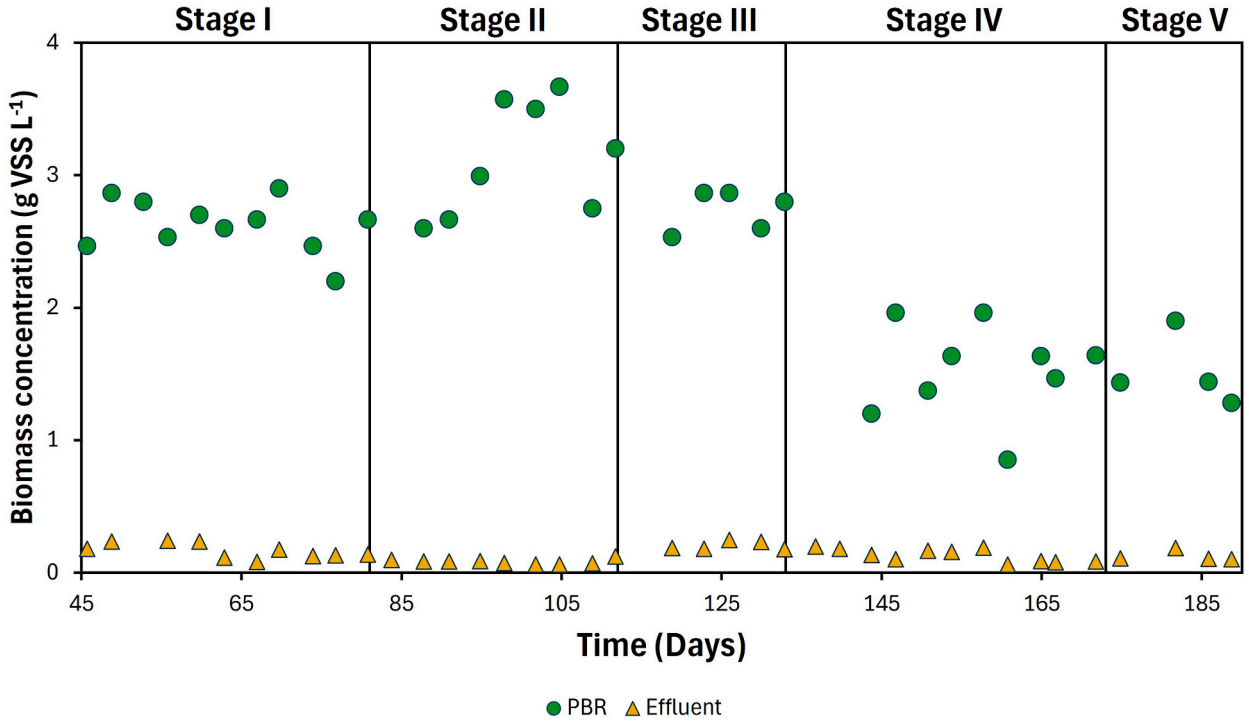


**Fig. 5.** Time course of the biomass concentration in gVSS $L^{-1}$ in the PBR and effluent through the study.

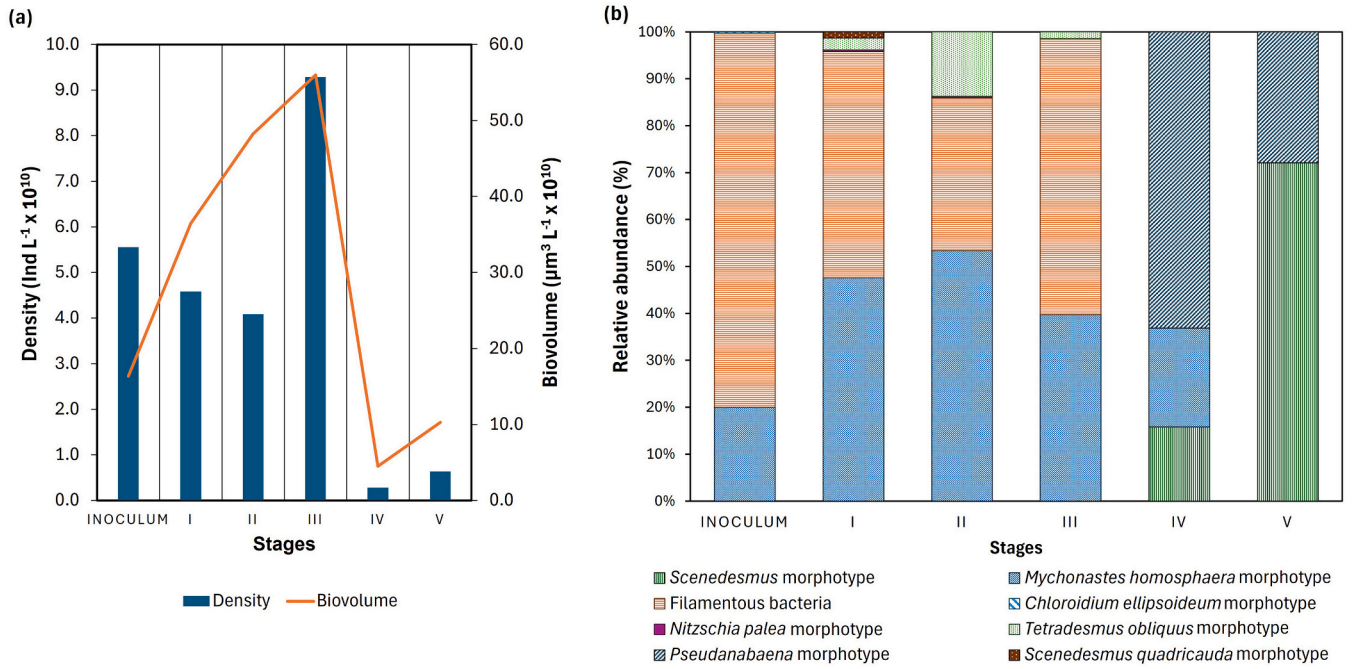


**Fig. 6.** Time course of (a) total microalgae densities and total microalgae biovolume, as estimated by microscopic analysis and (b) the relative abundances (%) per species of the main phyla of microalgae in the PBR during the operational stages.

concentration and density to their lowest recorded levels. Notably, *Pseudanabaena* morphotype showed the highest relative abundance (63 %) alongside *Mychonastes homosphaera* morphotype (21 %) and *Scenedesmus* sp. (16 %) morphotype. However, the period of enhanced light availability in Stage V was accompanied by a 126 % increase in cell density and a 129 % increase in biovolume, achieving the highest relative cell volume (16.2 $\mu m^3$ $cell^{-1}$) observed in the study. In stage V, *Scenedesmus* morphotype became the most prevalent (72 %), while *Pseudanabaena* morphotype abundance declined to 28 % and *Mychonastes homosphaera* morphotype was undetectable.

The enhanced S/V ratio in Stage V particularly favoured *Scenedesmus* morphotype potentially due to its reported tolerance to high light intensities compared to *Pseudanabaena* morphotype [10]. Interestingly, the reduced SRT in Stages IV and V was associated with decreased microalgal richness and diversity, particularly affecting filamentous bacteria. This observation aligns with previous studies showing that an extended SRT supports a broader range of growth parameters and microbial diversity [25,45].

## 4. Conclusion

This study demonstrated that a single-stage algal-bacterial photobioreactor achieved high removal efficiencies for ammonium (up to 99 %), total nitrogen (92–97 %), total organic carbon (up to 95 %) and phosphate (100 % in Stage V), alongside a biomass productivity of 336 $\pm$ 79 g $m^{-3}$ $d^{-1}$ by balancing the HRT, SRT, and light availability. The system maintained high bioremediation efficiency, comparable to more complex multi-stage systems, even at short HRTs (2 days), highlighting the potential of single-stage PBRs as an alternative for wastewater treatment, characterized by its operational simplicity inherent to a compact, single-tank design, high nutrient removal efficiency, and biomass production with biotechnological potential. Future research should focus on exploring the treatment of different effluents with varying C:N:P ratios to increase its applicability and scalability and to demonstrate the occurrence of simultaneous nitrification-denitrification in the algal-bacterial broth.

## CRediT authorship contribution statement

**Thalita Lacerda dos Santos:** Writing – original draft, Investigation, Conceptualization. **Laura Vargas-Estrada:** Writing – review & editing, Validation, Conceptualization. **Saúl Blanco:** Investigation, Formal analysis. **Gustavo Henrique Ribeiro da Silva:** Writing – review & editing, Supervision, Project administration, Funding acquisition. **Raúl Muñoz:** Writing – review & editing, Validation, Supervision, Resources, Project administration, Funding acquisition, Conceptualization.

## Declaration of competing interest

The authors declare that they have no known competing financial interests or personal relationships that could have appeared to influence the work reported in this paper.

## Acknowledgements

The scholarship granted by the Brazilian Federal Agency for Support and Evaluation of Graduate Education (CAPES), within the scope of CAPES-PrInt Program (Project number 88887.194785/2018-00; Process number 88887.892272/2023-00) is gratefully acknowledged. Laura Vargas-Estrada acknowledges the Marie Skłodowska-Curie Individual Fellowship (Grant Agreement No 101148763). The National Council for Scientific and Technological Development (CNPq; Process number 301994/2025–0) is gratefully acknowledged.

## Data availability

No data was used for the research described in the article.

## References

[1] S.F. Mohsenpour, S. Hennige, N. Willoughby, A. Adeloye, T. Gutierrez, Integrating micro-algae into wastewater treatment: a review, Sci. Total Environ. 752 (2021) 142168, https://doi.org/10.1016/j.scitotenv.2020.142168.
[2] F. Han, W. Zhou, Nitrogen recovery from wastewater by microbial assimilation – a review, Bioresour. Technol. 363 (2022) 127933, https://doi.org/10.1016/j.biortech.2022.127933.

[3] R.K. Oruganti, K. Katam, P.L. Show, V. Gadhamshetty, V.K.K. Upadhyayula, D. Bhattacharyya, A comprehensive review on the use of algal-bacterial systems for wastewater treatment with emphasis on nutrient and micropollutant removal, Bioengineered 13 (2022) 10412–10453, https://doi.org/10.1080/21655979.2022.2056823.
[4] M.E. Wali, S.R. Golroudbary, A. Kraslawski, Circular economy for phosphorus supply chain and its impact on social sustainable development goals, Sci. Total Environ. 777 (2021) 146060, https://doi.org/10.1016/j.scitotenv.2021.146060.
[5] Y. Yan, H. Lu, J. Zhang, S. Zhu, Y. Wang, Y. Lei, R. Zhang, L. Song, Simultaneous heterotrophic nitrification and aerobic denitrification (SND) for nitrogen removal: a review and future perspectives, Environ. Adv. 9 (2022) 100254, https://doi.org/10.1016/j.envadv.2022.100254.
[6] Q. Li, Y. Xu, C. Liang, L. Peng, Y. Zhou, Nitrogen removal by algal-bacterial consortium during mainstream wastewater treatment: transformation mechanisms and potential N2O mitigation, Water Res. 235 (2023) 119890, https://doi.org/10.1016/j.watres.2023.119890.
[7] C. Alcántara, E. Posadas, B. Guieysse, R. Muñoz, Microalgae-based Wastewater Treatment, 2015, pp. 439–455, https://doi.org/10.1016/b978-0-12-800776-1.00029-7.
[8] T.V. Fernandes, R. Shrestha, Y. Sui, G. Papini, G. Zeeman, L.E.M. Vet, R.H. Wijffels, P. Lamers, Closing domestic nutrient cycles using microalgae, Environ. Sci. Technol. 49 (2015) 12450–12456, https://doi.org/10.1021/acs.est.5b02858.
[9] P. Foladori, S. Petrini, G. Andreottola, How suspended solids concentration affects nitrification rate in microalgal-bacterial photobioreactors without external aeration, Heliyon 6 (2020) e03088, https://doi.org/10.1016/j.heliyon.2019.e03088.
[10] E. Posadas, C. Alcántara, P.A. García-Encina, L. Gouveia, B. Guieysse, Z. Norvill, F. G. Acién, G. Markou, R. Congestri, J. Koreiviene, R. Muñoz, 3 - microalgae cultivation in wastewater, in: C. Gonzalez-Fernandez, R. Muñoz (Eds.), Microalgae-Based Biofuels and Bioproducts, Woodhead Publishing, 2017, pp. 67–91, https://doi.org/10.1016/B978-0-08-101023-5.00003-0.
[11] G. Kwon, H. Kim, C. Song, D. Jahng, Co-culture of microalgae and enriched nitrifying bacteria for energy-efficient nitrification, Biochem. Eng. J. 152 (2019) 107385, https://doi.org/10.1016/j.bej.2019.107385.
[12] A. Karemore, D. Ramalingam, G. Yadav, G. Subramanian, R. Sen, Photobioreactors for improved algal biomass production: analysis and design considerations, in: D. Das (Ed.), Algal Biorefinery: An Integrated Approach, Springer International Publishing, Cham, 2015, pp. 103–124, https://doi.org/10.1007/978-3-319-22813-6_5.
[13] A.F. Torres-Franco, M. Zuluaga, D. Hernández-Roldán, D. Leroy-Freitas, C. A. Sepúlveda-Muñoz, S. Blanco, C.R. Mota, R. Muñoz, Assessment of the performance of an anoxic-aerobic microalgal-bacterial system treating digestate, Chemosphere 270 (2021) 129437, https://doi.org/10.1016/j.chemosphere.2020.129437.
[14] L. Vargas-Estrada, A. Longoria, P.U. Okoye, P.J. Sebastian, Energy and nutrients recovery from wastewater cultivated microalgae: assessment of the impact of wastewater dilution on biogas yield, Bioresour. Technol. 341 (2021) 125755, https://doi.org/10.1016/j.biortech.2021.125755.
[15] C. Alcántara, E. Posadas, B. Guieysse, R. Muñoz, Microalgae-based wastewater treatment, in: S.-K. Kim (Ed.), Handbook of Marine Microalgae, Academic Press, Boston, 2015, pp. 439–455, https://doi.org/10.1016/B978-0-12-800776-1.00029-7.
[16] A.M. Rada-Ariza, D. Fredy, C.M. Lopez-Vazquez, N.P. Van der Steen, P.N.L. Lens, Ammonium removal mechanisms in a microalgal-bacterial sequencing-batch photobioreactor at different solids retention times, Algal Res. 39 (2019) 101468, https://doi.org/10.1016/j.algal.2019.101468.
[17] X. Zhong, H. Zhao, S. Yue, J. Fan, Algal-bacterial consortia driven nitrite accumulation and phosphorus removal in partial denitrification, J Water Process Eng 68 (2024) 106504, https://doi.org/10.1016/j.jwpe.2024.106504.
[18] Z. Arbib, J. Ruiz, P. Álvarez-Díaz, C. Garrido-Pérez, J. Barragan, J.A. Perales, Effect of pH control by means of flue gas addition on three different photo-bioreactors treating urban wastewater in long-term operation, Ecol. Eng. 57 (2013) 226–235, https://doi.org/10.1016/j.ecoleng.2013.04.040.
[19] G.A. Andrade, M. Berenguel, J.L. Guzmán, D.J. Pagano, F.G. Acién, Optimization of biomass production in outdoor tubular photobioreactors, J. Process Control 37 (2016) 58–69, https://doi.org/10.1016/j.jprocont.2015.10.001.
[20] M.C. Deprá, L.G.R. Mérida, C.R. de Menezes, L.Q. Zepka, E. Jacob-Lopes, A new hybrid photobioreactor design for microalgae culture, Chem. Eng. Res. Des. 144 (2019) 1–10, https://doi.org/10.1016/j.cherd.2019.01.023.
[21] Z. Arbib, J. Ruiz, P. Álvarez-Díaz, C. Garrido-Pérez, J. Barragan, J.A. Perales, Long term outdoor operation of a tubular airlift pilot photobioreactor and a high rate algal pond as tertiary treatment of urban wastewater, Ecol. Eng. 52 (2013) 143–153, https://doi.org/10.1016/j.ecoleng.2012.12.089.
[22] J. González-Camejo, S. Aparicio, M. Pachés, L. Borrás, A. Seco, Comprehensive assessment of the microalgae-nitrifying bacteria competition in microalgae-based wastewater treatment systems: relevant factors, evaluation methods and control strategies, Algal Res. 61 (2022) 102563, https://doi.org/10.1016/j.algal.2021.102563.
[23] Q. Meng, W. Zeng, J. Zhang, H. Liu, S. Li, Y. Peng, Combined phototrophic simultaneous nitrification-endogenous denitrification with phosphorus removal (P-SNDPR) system treating low carbon to nitrogen ratio wastewater for potential carbon neutrality, Environ. Sci. Technol. 58 (2024) 2902–2911, https://doi.org/10.1021/acs.est.3c09351.
[24] Shinichi Akizuki, S. Akizuki, Masatoshi Kishi, M. Kishi, Germán Cuevas-Rodríguez, G. Cuevas-Rodríguez, Tatsuki Toda, T. Toda, Corrigendum to "Effects of different light conditions on ammonium removal in a consortium of microalgae and partial nitrifying granules" [Water Res. 171 (2020) 115445], Water Res. 175 (115778) (2020), https://doi.org/10.1016/j.watres.2020.115778.
[25] M. Zhi, Z. Zhou, C. Yang, Y. Chen, Y. Xiao, F. Meng, Solid retention time regulates partial nitrification by algal-bacterial consortia in wastewater treatment: performance and mechanism, Chem. Eng. J. 452 (2023) 139537, https://doi.org/10.1016/j.cej.2022.139537.
[26] E.G. Hoyos, R. Kuri, T. Toda, R. Muñoz, Innovative design and operational strategies to improve CO2 mass transfer during photosynthetic biogas upgrading, Bioresour. Technol. 391 (2024) 129955, https://doi.org/10.1016/j.biortech.2023.129955.
[27] L. Ferro, M. Colombo, E. Posadas, C. Funk, R. Muñoz, Elucidating the symbiotic interactions between a locally isolated microalga Chlorella vulgaris and its co-occurring bacterium Rhizobium sp. in synthetic municipal wastewater, J. Appl. Phycol. 31 (2019) 2299–2310, https://doi.org/10.1007/s10811-019-1741-1.
[28] A. Solimeno, F.G. Acíen, J. García, Mechanistic model for design, analysis, operation and control of microalgae cultures: calibration and application to tubular photobioreactors, Algal Res. 21 (2017) 236–246, https://doi.org/10.1016/j.algal.2016.11.023.
[29] C. Alcántara, J.M. Domínguez, D. García, S. Blanco, R. Pérez, P.A. García-Encina, R. Muñoz, Evaluation of wastewater treatment in a novel anoxic–aerobic algal–bacterial photobioreactor with biomass recycling through carbon and nitrogen mass balances, Bioresour. Technol. 191 (2015) 173–186, https://doi.org/10.1016/j.biortech.2015.04.125.
[30] Standard Methods for the Examination of Water and Wastewater, American Public Health Association, 2017, https://doi.org/10.2105/SMWW.2882.
[31] O.D. Frutos, I.A. Arvelo, R. Pérez, G. Quijano, R. Muñoz, Continuous nitrous oxide abatement in a novel denitrifying off-gas bioscrubber, Appl. Microbiol. Biotechnol. 99 (2015) 3695–3706, https://doi.org/10.1007/s00253-014-6329-8.
[32] A. Toledo-Cervantes, E. Posadas, I. Bertol, S. Turiel, A. Alcoceba, R. Muñoz, Assessing the influence of the hydraulic retention time and carbon/nitrogen ratio on urban wastewater treatment in a new anoxic-aerobic algal-bacterial photobioreactor configuration, Algal Res. 44 (2019) 101672, https://doi.org/10.1016/j.algal.2019.101672.
[33] S. Aparicio, L. Borrás-Falomir, A. Jiménez-Benítez, A. Seco, Á. Robles, Urban wastewater treatment at ambient conditions using microalgae-bacteria consortia in a membrane high-rate algal pond (MHRAP): the effect of hydraulic retention time and influent strength, Environ. Technol. Innov. 36 (2024) 103846, https://doi.org/10.1016/j.eti.2024.103846.
[34] J. Arango, A. Rojo, F. Casagli, O. Bernard, D. Jeison, Assessing the impact of biomass retention in membrane-assisted microalgae-bacteria sewage treatment, J. Environ. Chem. Eng. 13 (2025) 118546, https://doi.org/10.1016/j.jece.2025.118546.
[35] P.J. He, B. Mao, F. Lü, L.M. Shao, D.J. Lee, J.S. Chang, The combined effect of bacteria and *Chlorella vulgaris* on the treatment of municipal wastewaters, Bioresour. Technol. 146 (2013) 562–568, https://doi.org/10.1016/j.biortech.2013.07.111.
[36] E. Posadas, P.-A. García-Encina, A. Soltau, A. Domínguez, I. Díaz, R. Muñoz, Carbon and nutrient removal from centrates and domestic wastewater using algal-bacterial biofilm bioreactors, Bioresour. Technol. 139 (2013) 50–58, https://doi.org/10.1016/j.biortech.2013.04.008.
[37] C. González, J. Marciniak, S. Villaverde, C. León, P.A. García, R. Muñoz, Efficient nutrient removal from swine manure in a tubular biofilm photo-bioreactor using algae-bacteria consortia, Water Sci. Technol. 58 (2008) 95–102, https://doi.org/10.2166/wst.2008.655.
[38] D.M. Buha, K.R. Atalia, N.K. Shah, Continuous process study on simultaneous nitrification–denitrification of high ammoniacal nitrogen load wastewater in aerobic–anoxic sequencing bioreactors, Int. J. Environ. Sci. Technol. 14 (2017) 2451–2458, https://doi.org/10.1007/s13762-017-1333-z.
[39] J. González-Camejo, S. Aparicio, M.V. Ruano, L. Borrás, R. Barat, J. Ferrer, Effect of ambient temperature variations on an indigenous microalgae-nitrifying bacteria culture dominated by *Chlorella*, Bioresour. Technol. 290 (2019) 121788, https://doi.org/10.1016/j.biortech.2019.121788.
[40] D. de Haas, J. Andrews, Nitrous oxide emissions from wastewater treatment - revisiting the IPCC 2019 refinement guidelines, Environ. Chall. 8 (2022) 100557, https://doi.org/10.1016/j.envc.2022.100557.
[41] Y. Jo, E.G. Hoyos, S. Blanco, S.-H. Kim, R. Muñoz, Assessing nitrous oxide emissions from algal-bacterial photobioreactors devoted to biogas upgrading and digestate treatment, Chemosphere 361 (2024) 142528, https://doi.org/10.1016/j.chemosphere.2024.142528.
[42] A.F. Esteves, E.M. Salgado, V.J.P. Vilar, A.L. Gonçalves, J.C.M. Pires, A growth phase analysis on the influence of light intensity on microalgal stress and potential biofuel production, Energy Convers. Manag. 311 (2024) 118511, https://doi.org/10.1016/j.enconman.2024.118511.
[43] I. de Godos, V.A. Vargas, H.O. Guzmán, R. Soto, B. García, P.A. García, R. Muñoz, Assessing carbon and nitrogen removal in a novel anoxic–aerobic cyanobacterial–bacterial photobioreactor configuration with enhanced biomass sedimentation, Water Res. 61 (2014) 77–85, https://doi.org/10.1016/j.watres.2014.04.050.
[44] A. Toledo-Cervantes, M.L. Serejo, S. Blanco, R. Pérez, R. Lebrero, R. Muñoz, Photosynthetic biogas upgrading to bio-methane: boosting nutrient recovery via biomass productivity control, Algal Res. 17 (2016) 46–52, https://doi.org/10.1016/j.algal.2016.04.017.
[45] C. Mansfeldt, S. Achermann, Y. Men, J.-C. Walser, K. Villez, A. Joss, D.R. Johnson, K. Fenner, Microbial residence time is a controlling parameter of the taxonomic composition and functional profile of microbial communities, ISME J. 13 (2019) 1589–1601, https://doi.org/10.1038/s41396-019-0371-6.